Apoptosis induction via microtubule disassembly by an antitumour compound, pironetin

Masuo KONDOH*†[1], Takeo USUI*, Takaaki NISHIKIORI‡, Tadanori MAYUMI† and Hiroyuki OSADA*[2]

*Antibiotics Laboratory, The Institute of Physical and Chemical Research (RIKEN), Hirosawa 2-1, Wako-shi, Saitama, 351-0198, Japan, †Faculty of Pharmaceutical Science, Osaka University, 1-6 Yamada-oka, Suita, Osaka, 565-0871, Japan, and ‡Bioresources Group, Nippon Kayaku Co. Ltd., 225-1 Koshikiya, Horigome, Ageo-shi, Saitama, 362-0064, Japan

We reported previously that pironetin and its derivatives were potent inhibitors of cell cycle progression at the M-phase and showed antitumour activity against a murine tumour cell line, P388 leukaemia, transplanted in mice. In this paper, we investigated the mechanism of action of pironetins in antitumour activity and cell cycle arrest at the M-phase. As reported previously for murine leukaemia P388 cells, pironetin showed antitumour activity in a dose-dependent manner in the human leukaemia cell line HL-60. Since DNA fragmentation was observed in both P388 and HL-60 cells, the antitumour activity of pironetin is thought to be due to the induction of apoptosis. Pironetin also induced the rapid phosphorylation of Bcl-2 before formation of the DNA ladder in HL-60 cells, as seen with several tubulin binders. These results suggest that the antitumour activity of pironetin is due to apoptosis caused by the phosphorylation of Bcl-2, and that pironetin targets the microtubules. Pironetin and demethylpironetin exhibited reversible disruption of the cellular microtubule network in normal rat fibroblast 3Y1 cells. However, epoxypironetin, which contains epoxide instead of the double bond of pironetin, showed only weak activity. Since the concentrations that inhibit cell cycle progression at the M-phase were the same as those for disruption of the microtubule network, it was suggested that the mitotic arrest induced by pironetin was the result of the loss of the mitotic spindle. These compounds also inhibited the microtubule-associated protein-induced and glutamate-induced tubulin assembly *in vitro*. Pironetin inhibited the binding of [^{3}H]vinblastine, but not that of [^{3}H]colchicine, to tubulin, and the K_d values revealed that the affinity of pironetin for tubulin is stronger than that of vinblastine. These results suggest that pironetins are novel antitumour agents which inhibit microtubule assembly.

Key words: microtubule network, programmed cell death, surface plasmon resonance, tubulin.

INTRODUCTION

Apoptosis is a cell suicide mechanism to eliminate damaged cells from multicellular organisms. It is well known that antitumour agents induce apoptosis through various signalling pathways in tumour cells. We have recently demonstrated that a novel antitumour agent, cytotrienin A, induced apoptosis in human leukaemia HL-60 cells through the generation of radical oxygen species [1]. Several groups have also reported that paclitaxel and vinblastine, antimicrotubule drugs with significant clinical activity, induce apoptosis in a variety of tumours [2–5].

It is known that Bcl-2 is a guardian of microtubule integrity [6]. The *Bcl-2* gene was discovered as a kind of oncogene involved in non-Hodgkin's B-cell lymphoma and it encoded an anti-apoptotic protein [7,8]. Bcl-2 and related anti-apoptotic proteins seem to dimerize with a pro-apoptotic molecule, such as Bax, inhibiting its function. It is thought that phosphorylation of Bcl-2 at serine residues leads to a loss of the Bcl-2 anti-apoptotic function and that the cells then execute apoptosis. Indeed, several groups reported that paclitaxel and other microtubule binders induce the phosphorylation of Bcl-2 followed by apoptosis in acute leukaemia and prostate cancer cell lines [6,9–12].

Drugs that interact with tubulin, the main constituent of microtubules, are not only antitumour agents, but are also useful tools for understanding a wide variety of the cellular functions of microtubules, which play important roles in mitosis, cell signalling and motility in eukaryotes. Paclitaxel and vinblastine bind different sites of tubulin and show opposite effects *in vitro*; paclitaxel induces microtubule bundling and vinblastine induces microtubule disassembly. We recently reported that tryprostatin A inhibited the microtubule-associated protein-dependent tubulin assembly by binding tubulin at different binding sites than do colchicine and vinblastine. The drugs bind to their own sites on the tubulin or microtubule-associated protein, suggesting that novel tubulin binding drugs will be discovered.

Previously, we reported that pironetin and its derivatives (Figure 1) were M-phase inhibitors and exhibited antitumour activity in a murine model [13]. However, the mode of action was unclear until now. Paclitaxel and vinblastine are anticancer drugs with significant clinical activity against a variety of tumours. It is known that both drugs induce cell cycle arrest at G2/M, which is followed by the DNA fragmentation and morphological features of apoptosis, in various human leukaemia cell lines. In this paper, we investigated the antitumour activity of pironetin in mouse leukaemia P388 cells and human leukaemia HL-60 cells, and found that pironetin induces apoptosis following the phosphorylation of Bcl-2. The effects of pironetin resembled those of other antitumour agents, which inhibit microtubule functions. We investigated the effect of pironetin and its derivatives, demethylpironetin and epoxypironetin, on microtubule

Abbreviation used: MTT, 3-(4,5-dimethylthiazol-2-yl)-2,5-diphenyl-2*H*-tetrazolium bromide.

[1] Present address: Faculty of Pharmaceutical Science, Tokushima Bunri University, 180 Yamashiro-cho, Tokushima, 770-8514, Japan.
[2] To whom correspondence should be addressed (e-mail antibiot@postman.riken.go.jp).

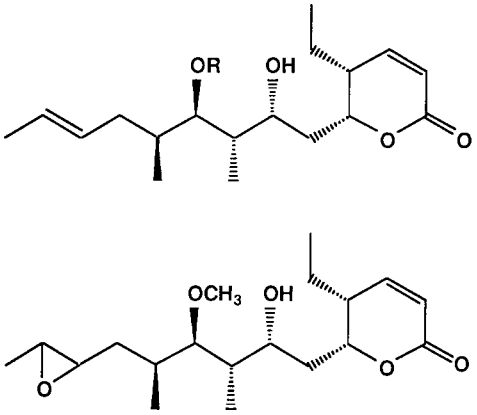

Figure 1 Structure of pironetin and its derivatives

Upper panel: R = CH_3 for pironetin and R = H for demethylpironetin. Lower panel: epoxypironetin.

and tubulin assembly *in situ* and *in vitro*, and found that these compounds were novel microtubule inhibitors.

MATERIALS AND METHODS

Materials

Pironetin and its derivatives were purified as described previously [14,15]. Colchicine and vinblastine were purchased from Sigma (St. Louis, MO, U.S.A.) and Wako Pure Chemical Industries Ltd. (Osaka, Japan) respectively. [^{3}H]Vinblastine and [^{3}H]colchicine were purchased from ICN Biomedicals Inc. (Costa Mesa, CA, U.S.A.) and NEN Life Science Products Inc. (Boston, MA, U.S.A.), respectively. Compounds were dissolved in DMSO.

Cell culture and cell viability assay

Murine leukaemia P388 cells and human myeloid leukaemia HL-60 cells were cultured to exponential growth phase in RPMI 1640 supplemented with 10 % (v/v) fetal-calf serum. Rat normal fibroblast 3Y1 cells were grown in Dulbecco's modified Eagle's (DMEM) medium supplemented with 10 % fetal-calf serum [16]. Both cell lines were cultured in a humidified atmosphere containing 5 % CO_2.

The antitumour activity of pironetin against HL-60 leukaemia cells was assessed as follows: 4×10^4 cells seeded on to 96-well plates were incubated with various drugs at the indicated concentrations at 37 °C for 24 or 48 h. The cell viability was determined using the colorimetric 3-(4,5-dimethylthiazol-2-yl)-2,5-diphenyl-2*H*-tetrazolium bromide (MTT) assay [17] with some modifications. Briefly, after the addition of 0.5 mg/ml MTT in PBS, cells were incubated at 37 °C for 4 h. SDS (10 %, w/v) in 0.05 M HCl was added to the wells and then incubated at room temperature for 6 h under dark conditions. The absorbance was measured at 595 nm.

DNA fragmentation assay

Cells were harvested by centrifugation (1500 ***g***) and washed with PBS. The washed cells were lysed with a lysis buffer [10 mM Tris/HCl, pH 8.0, 10 mM EDTA, 0.5 % (w/v) SDS and 0.1 % (w/v) RNase A] and incubated for 60 min at 50 °C. The lysate was incubated for an additional 60 min at 50 °C with 1 mg/ml proteinase K. DNA extraction was carried out and the purified samples were electrophoresed on a 1.8 % (w/v) agarose gel. After electrophoresis, the DNA was visualized by ethidium bromide staining.

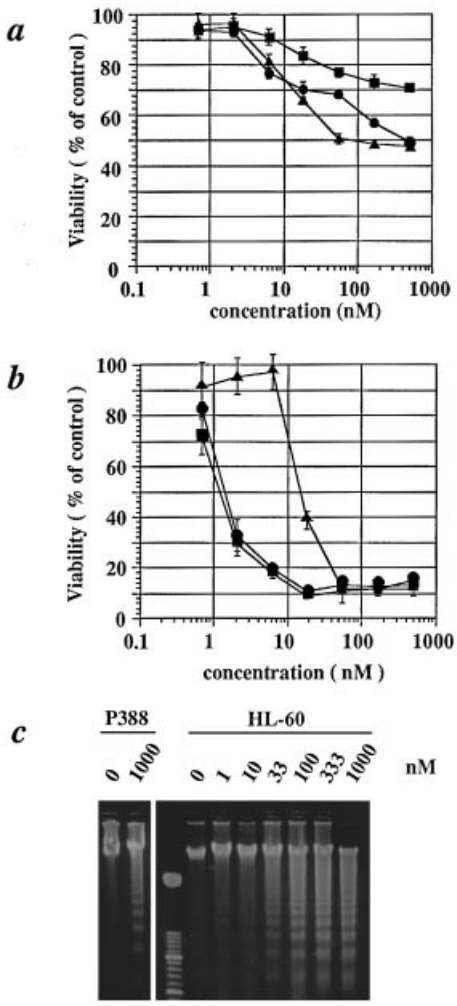

Figure 2 Effects of pironetin on cell proliferation and the induction of apoptosis

Exponentially growing (***a***) mouse leukaemia P388 and (***b***) human leukaemia HL-60 cells (1×10^6 cells/100 μl per well) were treated with various concentrations of mitotic inhibitors: pironetin (▲), vinblastine (●) and paclitaxel (■). After 24 h of treatment, the cells were harvested and the cytotoxic effects were determined using the MTT colorimetric method. (***c***) Internucleosomal fragmentation of pironetin-treated P388 and HL-60 cells. P388 cells were treated with 1 μM pironetin for 24 h and HL-60 cells were treated with various concentrations of pironetin for 18 h. After treatment, the cells were harvested and the isolated DNA was analysed by agarose gel electrophoresis.

Immunoblot analysis

Equal amounts of proteins extracted from control or drug-treated cells were subjected to SDS/PAGE [12.5 % (w/v) gel]. The proteins were transferred to a poly(vinylidene fluoride) membrane. The transferred proteins were subjected to immunoblotting using an anti-Bcl-2 monoclonal antibody (DAKO A/S, Glostrup, Denmark) and horseradish peroxidase-conjugated goat anti-mouse IgG (BioRad). The protein bands were visualized using the SuperSignal Substrate (Pierce, Rockford, IL, U.S.A.). The phosphorylated form of the Bcl-2 protein was detected as the slower mobility form [9].

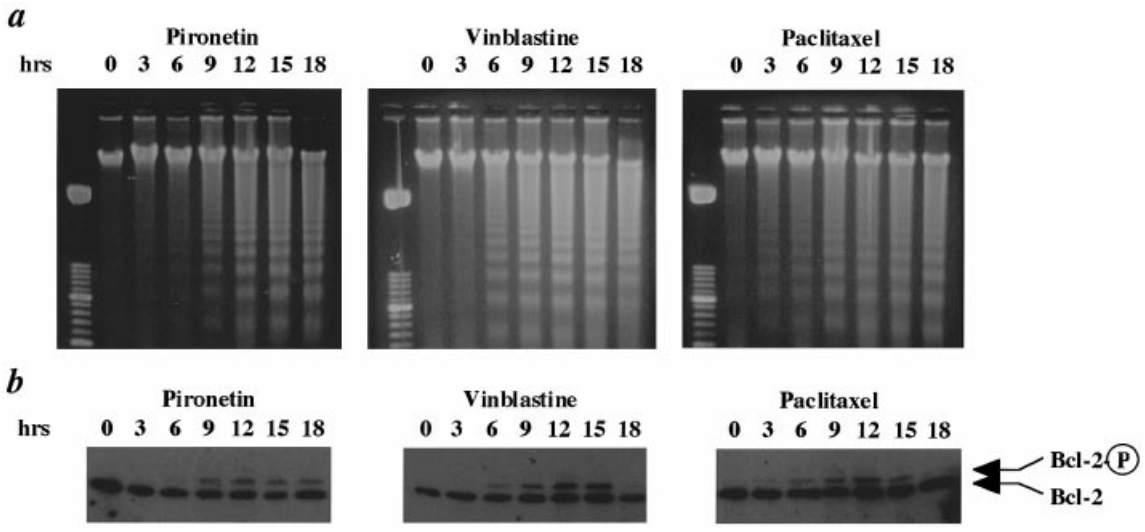

Figure 3 Phosphorylation of the Bcl-2 protein during apoptosis

(***a***) Time course of DNA fragmentation and (***b***) phosphorylation of the Bcl-2 protein in HL-60 cells treated with M-phase arresting compounds. Exponentially growing HL-60 cells were treated with 0.1% DMSO containing pironetin, vinblastine or paclitaxel (final concentrations were 33, 10 and 10 nM respectively). Treatment with 0.1% DMSO had no effect on the DNA fragmentation and phosphorylation of the Bcl-2 protein (results not shown). At the indicated times, the treated cells were collected and analysed as described in Materials and methods section.

Immunofluorescence procedures

Immunofluorescence observation of tubulin was performed as described in [18]. The cytoskeletons were photographed using a cooled charge-coupled device (CCD) camera (Olympus PROVIS AX70, Tokyo, Japan).

Preparation of microtubule and tubulin protein

Calf brain microtubule protein was prepared by two cycles of assembly/disassembly [19] and stored at −80 °C in Mes buffer [100 mM Mes, pH 6.8/1 mM EGTA/0.5 mM $MgCl_2$]. Tubulin was prepared by phosphocellulose (P11, Whatman, Kent, U.K.) column chromatography of microtubule proteins as the void fraction [20]. Protein concentrations were determined using the Protein Assay (BioRad, Hercules, CA, U.S.A.).

Turbidity assay

Microtubule and tubulin assembly were monitored by the turbidity assay described in [18]. In brief, microtubule protein (2.0 mg/ml in Mes buffer) or purified tubulin (0.5 mg/ml in Mes buffer containing 1 M glutamate, pH 6.8) was incubated at 37 °C and the change in absorbance at 350 nm was monitored with time. To examine the effect of pironetin on polymerization, the microtubule or tubulin protein was preincubated with 1% (v/v) DMSO containing various concentrations of pironetin at 0 °C and polymerization was initiated with the addition of 1 mM GTP on microtubule assembly or 4 mM GTP on tubulin assembly.

Binding assay

The competition assay of pironetin binding to tubulin with radiolabelled vinblastine or colchicine was monitored by the centrifugal gel filtration method described by Hamel and Lin [21]. A 1 ml Sephadex G-50 column (Superfine) was used.

To estimate the binding constant of pironetin, we used an SPR670 instrument (Nippon Laser & Electronics Lab., Nagoya, Japan), to measure the tubulin–compound interaction by surface plasmon resonance. Tubulin (10 mM in Mes buffer, pH 7.4) was fixed on to a sensor chip. Mes buffer, pH 7.4, was used to pass over the tubulin monolayer at 10 μl/min. The drugs were then injected and the signal changes were monitored. Kinetic constants were obtained from the analysis of sensorgram curves using kinetic evaluation software.

RESULTS

Pironetin induces apoptosis following the phosphorylation of Bcl-2 in HL-60 cells

As pironetin showed M-phase arrest and anticancer activity, we investigated whether this activity was due to apoptosis as it is in the cases of paclitaxel and vinblastine. The antiproliferative activity of pironetin in both mouse leukaemia P388 cells and human leukaemia HL-60 cells was determined by MTT assay (Figures 2*a* and 2*b*). Cell viability was drastically decreased by the 24 h treatment with pironetin, and the IC_{50} values were approx. 100 nM for P388 cells and 20 nM for HL-60 cells. P388 cells were also resistant, compared with HL-60 cells, to vinblastine and paclitaxel. Moreover, there were differences in drug sensitivity between P388 and HL-60 cells. P388 cells were sensitive to pironetin compared with paclitaxel; however, HL-60 cells were relatively resistant to pironetin. To evaluate whether the antiproliferative activity was due to apoptosis, we analysed DNA fragmentation, which is considered to be an important event of apoptosis. When P388 cells and HL-60 cells were treated with pironetin, a typical DNA ladder pattern of internucleosomal fragmentation was observed (Figure 2*c*). Although P388 cells required more than 500 nM pironetin for the induction of apoptosis (results not shown), 33 nM pironetin induced apoptosis in HL-60 cells. As HL-60 cells were more sensitive than P388 cells, we decided to use HL-60 cells for further analysis.

We investigated the phosphorylation of Bcl-2 and DNA fragmentation as a function of time. Pironetin (33 nM) induced

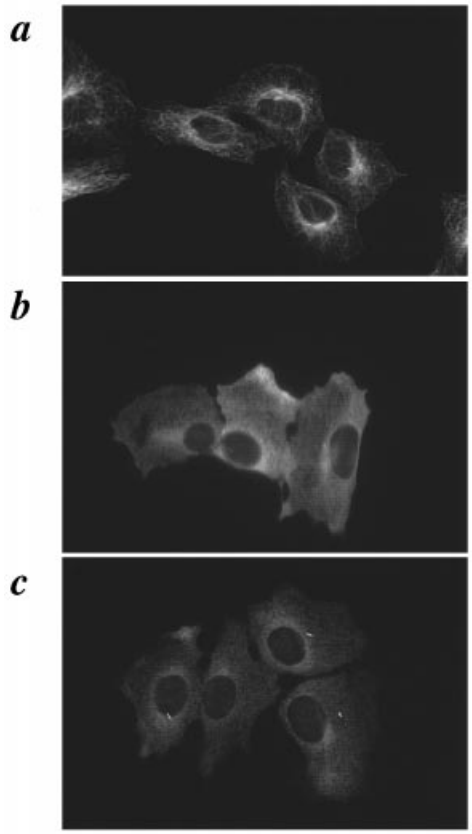

Figure 4 Reversible depolymerization of cellular microtubules by pironetin

Cellular microtubules in 3Y1 cells were observed using anti-α-tubulin antibody. (***a***) Control cells without drug treatment. 3Y1 cells incubated with (***b***) colchicine (1 μg/ml) or (***c***) pironetin (50 ng/ml) for 6 h.

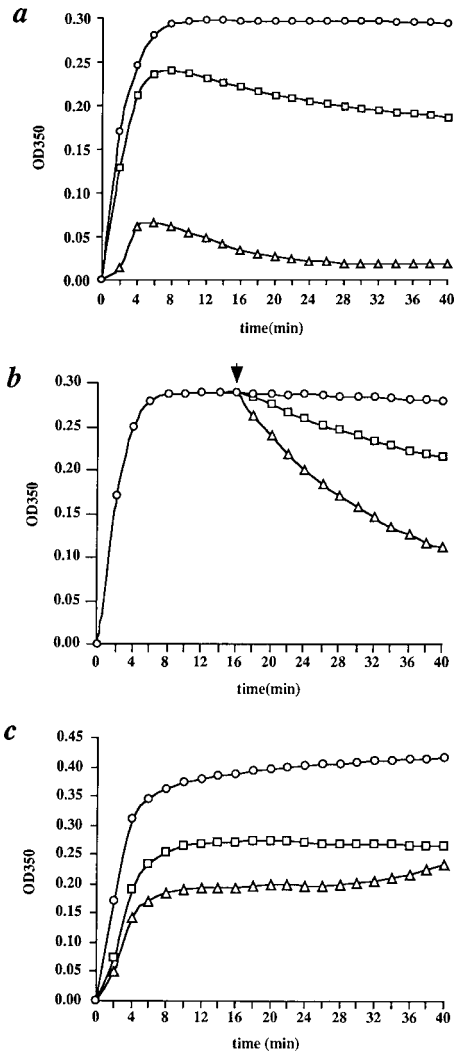

Figure 5 Effects of pironetin on microtubule assembly (*a*) and disassembly (*b*), and tubulin assembly (*c*) *in vitro*

(***a***) Microtubule proteins (2 mg/ml) were incubated with various concentrations of pironetin. The final concentrations of pironetin were 0 (○), 1 (□) and (△) 5 μg/ml respectively. (***b***) Microtubule proteins were assembled in the absence of pironetin. After 15 min (arrow) pironetin was added and disassembly was then monitored. The final concentrations of pironetin were 0 (○), 1 (□) and 5 (△) μg/ml respectively. (***c***) Tubulin (10 μM) was incubated with 1 M glutamate and 1 % DMSO containing various concentrations of pironetin. The final concentrations of pironetin were 0 (○), 10 (□) and 50 (△) μM respectively. OD350, Absorbance at 350 nm.

apoptosis in HL-60 cells after 9 h of treatment, and phosphorylation of Bcl-2 was observed 6 h after the addition of pironetin (Figure 3). Paclitaxel and vinblastine showed similar effects on HL-60 cells. These results suggest that the antitumour activity of pironetin is partly due to the induction of apoptosis by the phosphorylation of Bcl-2.

Pironetin disrupts the microtubule network *in situ*

The mechanism for the induction of apoptosis by pironetin resembles that of paclitaxel and vinblastine. Since both compounds are tubulin binders and impede microtubule function, we investigated the effect of pironetins on the cytoplasmic microtubule network of normal rat fibroblast 3Y1 cells by indirect fluorescence microscopy. Control cells showed a microtubule network, whereas colchicine, a potent inhibitor of microtubule assembly, disrupted the microtubule network completely (Figures 4*a* and 4*b*). Pironetin treatment also induced the disassembly of cytoplasmic microtubules at 20–50 nM in dose-dependent manner (Figure 4*c*), but did not induce the disassembly of the actin filaments (results not shown). This effect of pironetin on microtubule assembly was reversible, but the recovery of the network took a long time (about 12 h; results not shown).

Demethylpironetin induced microtubule disassembly at the same concentration as pironetin but epoxypironetin had only a weak effect (results not shown). The microtubule network was completely disrupted by epoxypironetin at a 50-fold higher concentration than that of pironetin. The difference in effective concentration against cellular microtubules between pironetin and its derivatives was also observed for cell cycle inhibition [13]. These results suggest that pironetin derivatives inhibit the cell cycle progression at the M-phase through the inhibition of microtubule assembly.

Pironetin inhibits microtubule and tubulin assembly *in vitro*

We investigated the effect of pironetin on microtubule assembly *in vitro* using the turbidity assay. Tubulin polymerization proceeded rapidly and reached a plateau in 5 min as shown in Figure 5(*a*). Pironetin inhibited tubulin polymerization in a dose-dependent manner and 15 μM pironetin inhibited it completely. The IC_{50} values for pironetin and demethylpironetin were almost

Table 1 Inhibitory effects of pironetin on the binding of colchicine and vinblastine to tubulin

The reaction mixture (0.35 ml) containing 0.5 mg/ml (approx. 5 μM) tubulin, 50 nM [^{3}H]vinblastine, 5% (v/v) DMSO and 50 μM mitotic inhibitor, was incubated for 5 min at room temperature. Aliquots (0.1 ml) were applied to triplicate columns of Sephadex G-50 and processed by centrifugal gel filtration.

	Radiolabelled drug bound (% of control)	
Drug	[^{3}H]Colchicine	[^{3}H]Vinblastine
Colchicine	49.0	150.0
Vinblastine	139.3	63.1
Pironetin	148.4	59.3

Table 2 Kinetic constants for mitotic inhibitors of tubulin

The apparent dissociation constant (K_d) was calculated using the relationship, $K_d = k_{diss}/k_{ass}$. The rate constants were determined from sensorgram curves using kinetic evaluation software.

	Surface plasmon resonance measurement		
Drug	K_d (M)	k_{ass} ($M^{-1} \cdot s^{-1}$)	k_{diss} (s^{-1})
Pironetin	3.3×10^{-7}	2.0×10^{4}	6.8×10^{-3}
Vinblastine	1.5×10^{-6}	4.2×10^{3}	6.4×10^{-3}
Tryprostatin A	1.1×10^{-3}	5.3×10^{0}	6.0×10^{-3}

the same and estimated to be 5 μM; however, epoxypironetin showed only weak inhibitory activity and the IC_{50} value was above 30 μM (results not shown). Pironetin inhibited the polymerization of tubulin and also induced disassembly of tubulin already polymerized. (Figure 5*b*). The newly reached equilibrium was almost the same as that observed for microtubules treated with pironetin at zero time.

To determine the effect of pironetin on the assembly of purified tubulin we investigated tubulin self-assembly *in vitro*, induced by the artificial inducer glutamate (Figure 5*c*). Pironetin, demethylpironetin and epoxypironetin inhibited the assembly of purified tubulin and the IC_{50} values were calculated to be approx. 10, 10 and 50 μM respectively. Since these concentrations parallel those for microtubule disassembly, the differences in the concentrations having inhibitory effects between the compounds is thought to be due to the effects on tubulin. To investigate the binding site of pironetin on tubulin, we conducted competition binding experiments with [^{3}H]vinblastine and [^{3}H]colchicine. Unlabelled vinblastine and colchicine decreased the binding of radiolabelled colchicine and vinblastine respectively (Table 1). Tryprostatin A did not interfere with the binding of radiolabelled compounds [18]. However, pironetin decreased the binding of [^{3}H]vinblastine and slightly increased the binding of [^{3}H]colchicine, as seen with vinblastine. The interaction of compounds and tubulin was also analysed by the surface plasmon resonance method. The results of real time analysis are summarized in Table 2. However, all three compounds showed almost the same dissociation rate constant (k_{diss}); the dissociation constant, K_d ($K_d = k_{diss}/k_{ass}$), for tryprostatin A was extremely high. The high K_d value was coincident with the weak inhibitory effect of tryprostatin A. On the contrary, pironetin showed a lower K_d value compared with vinblastine.

DISCUSSION

Paclitaxel and vinblastine show potent antitumour activities that are due to the induction of apoptosis by the phosphorylation of Bcl-2 [6,10,12]. Here, we examined whether the antitumour effect of pironetin was due to apoptosis in mouse leukaemia P388 cells and human leukaemia HL-60 cells. Pironetin induced apoptosis in a dose- (Figure 2*c*) and time-dependent manner (Figure 3*a*). Bcl-2 phosphorylation was observed prior to the appearance of a DNA fragmentation ladder (Figure 3*b*). These results suggest that pironetin, like other microtubule inhibitors, induces the phosphorylation of Bcl-2 and that the cells then execute apoptosis.

As the apoptosis-inducing activity of pironetin resembled that of tubulin binders, such as paclitaxel and vinblastine, we investigated the effects of pironetins on the microtubule network *in situ* and *in vitro*. Pironetin and its derivatives induced microtubule disassembly *in situ* (Figure 4). The concentrations of pironetin, demethylpironetin and epoxypironetin that induced microtubule disassembly *in situ* were 50, 50 and 1250 nM respectively. Since these concentrations were almost the same as the concentrations which were required for arresting cell cycle progression at the M-phase, M-phase specific inhibition may be due to interference with the function of the spindle apparatus, via the disassembly of microtubules [13]. Pironetin and its derivatives also inhibited both microtubule-associated protein-dependent and glutamate-induced tubulin assembly *in vitro* (Figures 5*a* and 5*c*). In the glutamate-induced tubulin assembly assay, the IC_{50} values for pironetin and demethylpironetin were approx. 10 μM, whereas the value for epoxypironetin was approx. 50 μM. It was thought that the weak activity of epoxypironetin *in situ* was due to the weak effect on tubulin. Pironetin also induced the disassembly of the pre-polymerized microtubules (Figure 5*b*). The same effect was observed on vinblastine treatment (results not shown). Furthermore, in the competition binding assay, pironetin showed a vinblastine-like competition pattern, that is, pironetin inhibited the binding of [^{3}H]vinblastine and promoted the binding of [^{3}H]colchicine to tubulin (Table 1). These results suggest that pironetin and its derivatives directly bind tubulin and inhibit the tubulin assembly in a vinblastine-like manner.

Pironetin and its derivatives have unique structures, containing only one pyran residue and an alkyl chain, that are simple compared with other M-phase inhibitors. They induced the disassembly of microtubules *in situ* and *in vitro*. Pironetin exhibited antitumour activity by the induction of apoptosis through the phosphorylation of Bcl-2. Although the effective dose of pironetin was slightly higher than that of vinblastine, with respect to its cytotoxicity to HL-60 cells, the K_d value, determined by the surface plasmon resonance method, was 10-fold lower than that of vinblastine (Table 2). These data indicate that the affinity of pironetin for tubulin was greater than that of vinblastine, but that the membrane permeability to pironetin of HL-60 cells may be less than that of vinblastine. The distinctive features of pironetin, compared with known tubulin binding agents, suggest that it is possible to create a new cancer therapy drug from pironetin as a lead compound, and by using adequate drug delivery systems.

We thank Dr. Ohmori for material purification and useful discussion. This work was supported by a Grant for Multibioprobe/Biodesign (RIKEN) and by a Grant from the Ministry of Education, Science, Sports and Culture, Japan.

REFERENCES

1 Kakeya, H., Onose, R. and Osada, H. (1998) Cancer Res. **58**, 4888–4894
2 Ling, Y. H., Yang, Y., Tornos, C., Singh, B. and Perez-Soler, R. (1998) Cancer Res. **58**, 3633–3640

3 Srivastava, R. K., Srivastava, A. R., Korsmeyer, S. J., Nesterova, M., Cho-Chung, Y. S. and Longo, D. L. (1998) Mol. Cell. Biol. **18**, 3509–3517
4 Wang, T. H., Wang, H. S., Ichijo, H., Giannakakou, P., Foster, J. S., Fojo, T. and Wimalasena, J. (1998) J. Biol. Chem. **273**, 4928–4936
5 Blagosklonny, M. V., Giannakakou, P., el-Deiry, W. S., Kingston, D. G., Higgs, P. I., Neckers, L. and Fojo, T. (1997) Cancer Res. **57**, 130–135
6 Haldar, S., Basu, A. and Croce, C. M. (1997) Cancer Res. **57**, 229–233
7 Tsujimoto, Y., Finger, L. R., Yunis, J., Nowell, P. C. and Croce, C. M. (1984) Science **226**, 1097–1099
8 Vaux, D. L., Cory, S. and Adams, J. M. (1988) Nature (London) **335**, 440–442
9 Haldar, S., Jena, N. and Croce, C. M. (1995) Proc. Natl. Acad. Sci. U.S.A. **92**, 4507–4511
10 Haldar, S., Chintapalli, J. and Croce, C. M. (1996) Cancer Res. **56**, 1253–1255
11 Haldar, S., Basu, A. and Croce, C. M. (1998) Cancer Res. **58**, 1609–1615
12 Srivastava, R. K., Srivastava, A. R., Korsmeyer, S. J., Nesterova, M., Cho-Chung, Y. S. and Longo, D. L. (1998) Mol. Cell. Biol. **18**, 3509–3517
13 Kondoh, M., Usui, T., Kobayashi, S., Tsuchiya, K., Nishikawa, K., Nishikiori, T., Mayumi, T. and Osada, H. (1998) Cancer Lett. **126**, 29–32
14 Kobayashi, S., Tsuchiya, K., Harada, T., Nishide, M., Kurokawa, T., Nakagawa, T., Shimada, N. and Kobayashi, K. (1994) J. Antibiot. (Tokyo) **47**, 697–702
15 Tsuchiya, K., Kobayashi, S., Nishikiori, T., Nakagawa, T. and Tatsuta, K. (1997) J. Antibiot. (Tokyo) **50**, 259–260
16 Kimura, G., Itagaki, A. and Summers, J. (1975) Int. J. Cancer **15**, 694–706
17 Mosmann, T. (1983) J. Immunol. Methods **65**, 55–63
18 Usui, T., Kondoh, M., Cui, C. B., Mayumi, T. and Osada, H. (1998) Biochem. J. **333**, 543–548
19 Shelanski, M. L., Gaskin, F. and Cantor, C. R. (1973) Proc. Natl. Acad. Sci. U.S.A. **70**, 765–768
20 Weingarten, M. D., Lockwood, A. H., Hwo, S. Y. and Kirschner, M. W. (1975) Proc. Natl. Acad. Sci. U.S.A. **72**, 1858–1862
21 Hamel, E. and Lin, C. M. (1984) J. Biol. Chem. **259**, 11060–11069

Received 23 November 1998/22 February 1999; accepted 12 March 1999